TI Designs:

Noise-immune Capacitive Proximity Sensor System Reference Design

TI Designs

TI Designs provide the foundation that you need including methodology, testing and design files to quickly evaluate and customize the system. TI Designs help ***you*** accelerate your time to market.

Design Resources

TIDA-00466	Design Folder
FDC2214	Product Folder
TPS61029	Product Folder
MSP430FR5969	Product Folder
CSD25310Q2	Product Folder

TI E2E™ Community

Ask The Analog Experts
WEBENCH® Design Center

Design Features

- Utilizes the FDC2214 EMI-resistant architecture
- Demonstrates proximity and capacitive touch button functionality
- Optimized to achieve maximum sensing distance and responsive button press detection
- Integrates FDC2214, MSP430FR5969, and TPS61029
- Standalone system powered via one AA-battery
- Firmware includes derivative-integration algorithm to process raw data

Featured Applications

- Industrial: control panels, thermostats
- Consumer: battery operated proximity wakeup systems

Block Diagram

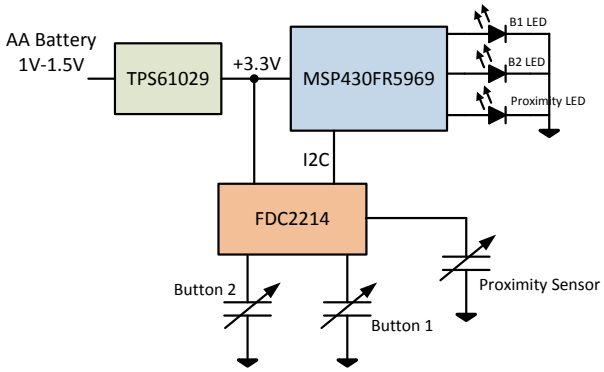

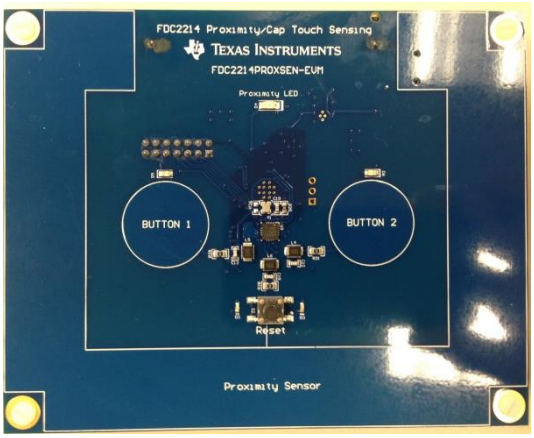

Table of Contents

1 Key System Specifications

Table 1: Key System Specifications

PARAMETER	SPECIFICATION	DETAILS
Sensor size	59cm^2	Section 4.3.2
Sensor configuration	Bezel Configuration	Section 4.3
Proximity Sensitivity (Sensing Distance)	10cm	Section 4.3.2
Sensor Frequency	5MHz	Section 8.1
Proximity Sensor Sampling Period	16ms	Section 8.1
Capacitive Touch Button Sampling Period	400us	Section 8.1

2 System Description

The FDC2214 proximity and capacitive touch button board demonstrates the use of TI's capacitive sensing technology to sense and measure the presence of various objects. The board is a complete hardware and firmware solution that integrates the FDC2214, MSP430FR5969, and TPS61029 into one design. The firmware included processes the data from one proximity sensor and two capacitive touch buttons via the FDC2214 to determine whether an object is in the intended sensing area. All of the processing is done on the MSP430 allowing the board to be a standalone system. Dedicated colored LEDs light up once the device detects a target in close proximity to the board or detects a press on the buttons. The board is designed to operate with one AA-battery. The maximum sensing distance that can be reliably achieved with the board is 10cm (4 inches) as a floating system and 50cm (19.6 inches) as a grounded system. The cap touch buttons and firmware have been optimized to be very responsive to quick user touch interactions.

The hardware utilizes the 4-channel FDC2214 to multiplex through each of the three capacitive sensors: one proximity sensor and two capacitive touch buttons. As the firmware in the MSP430 detects a user approaching the board, a green LED will light up to indicate that an object has been detected. If the user touches Button1, Button2, or both of them simultaneously, their corresponding red LED will light up. The board integrates the FDC2214, MSP430FR5969 and the TPS61029 as a complete standalone system. Figure 1 shows the top side of the reference design.

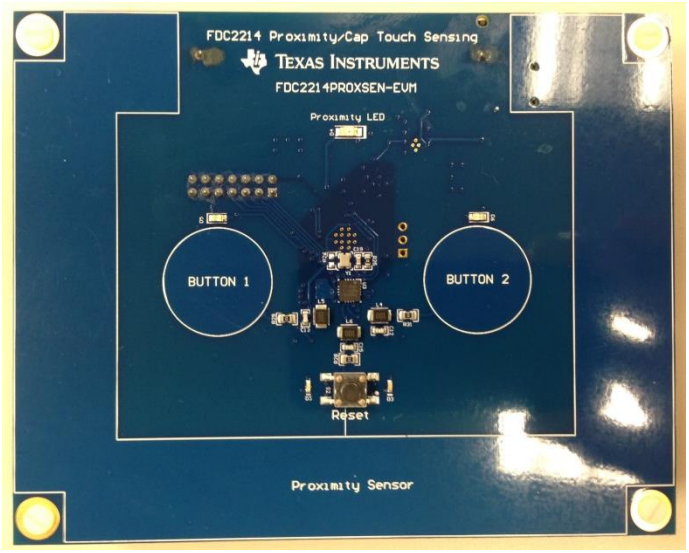

Figure 1: Proximity and capacitive touch sensing reference design

3 Block Diagram

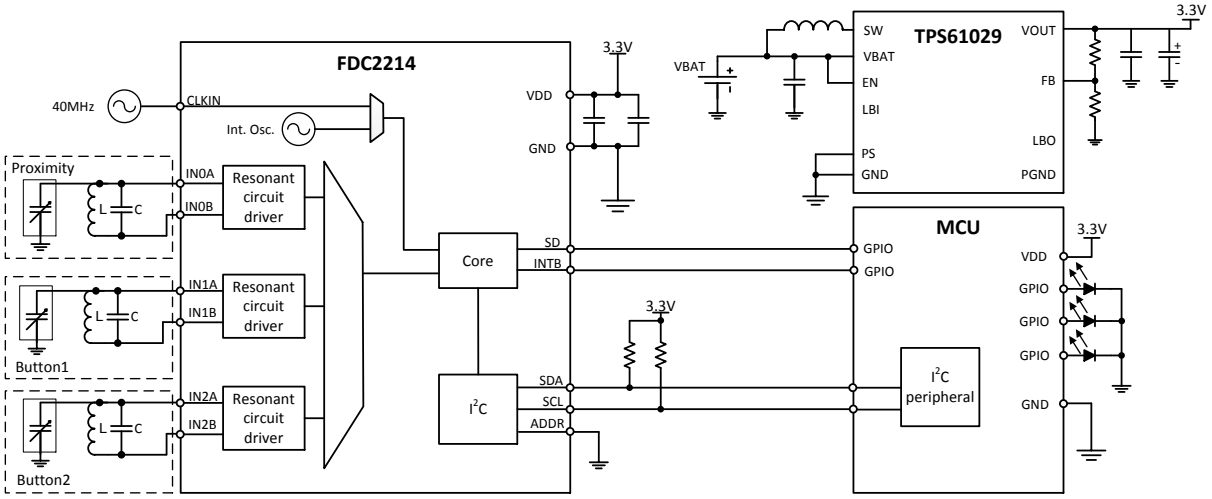

Figure 2: System level block diagram

3.1 Highlighted Products

The Proximity and Capacitive Touch Sensing reference design features the following devices:

- FDC2214: Four-channel capacitance-to-digital converter for capacitive sensing solutions
- TPS61029: 96% efficiency boost converter with a wide input voltage range suitable for one-cell battery applications
- MSP430FR5969: 16-MHz ULP microcontroller featuring 64-KB FRAM, 2-KB SRAM, 40 I/O

Dedicated LEDs are used to indicate whether an object has been detected in one of the respectively sensing areas.

3.1.1 FDC2214

The FDC2214 device employs an innovative narrow-band based architecture to offer high rejection of noise and interferers while providing high resolution at high sampling rates. The device supports a wide excitation frequency range, offering flexibility in system design. Some of the main features of the FDC2214 include:

- Maximum output rate (one active channel): 4.08ksps
- Maximum input capacitance: 250nF (at 10kHz with 1mH inductor)
- Sensor excitation frequency: 10kHz to 10MHz
- Resolution: up to 28bits
- System Noise Floor: 0.3fF at 100sps
- Supply voltage: 2.7V to 3.6V
- Power Consumption: 2.1mA active
- Low-power sleep mode: 35uA
- Shutdown: 200nA
- Interface: I^2C

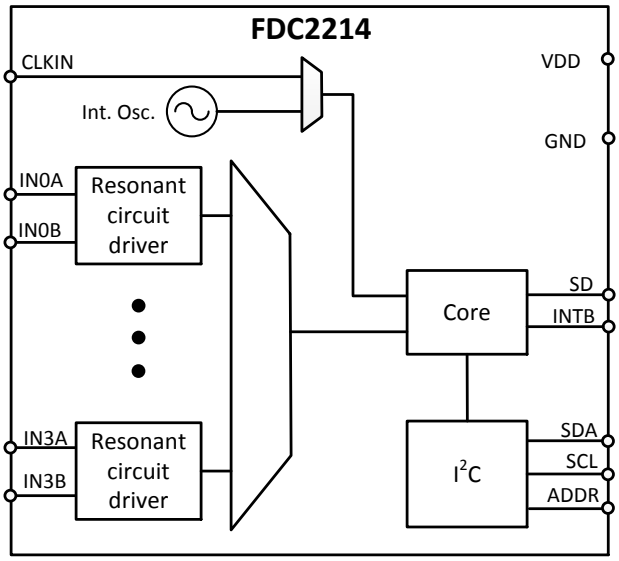

Figure 3: FDC2214 functional block diagram

3.1.2 TPS61029

The TPS61029 is a boost converter that can be powered by either one-cell, two-cell, or three-cell alkaline NiCd or NiMH, or one-cell Li-Ion or Li-polymer battery. Output current can go as high as 200mA while using a single-cell alkaline battery, and can maintain its output voltage as the battery discharges down to 0.9V. At low load currents, the converter enters the power save mode to maintain a high efficiency over a wide-load current range. Some of the main features of the TPS61029 include:

- Input Voltage Range: 0.9V to 6.5V
- Output Voltage Range: Adjustable
- Output Current: 1.8A peak
- Power Save Mode for Improved Efficiency at Low Output Power
- Device Quiescent Current: 25µA
- Low Battery Comparator
- Load Disconnect During Shutdown

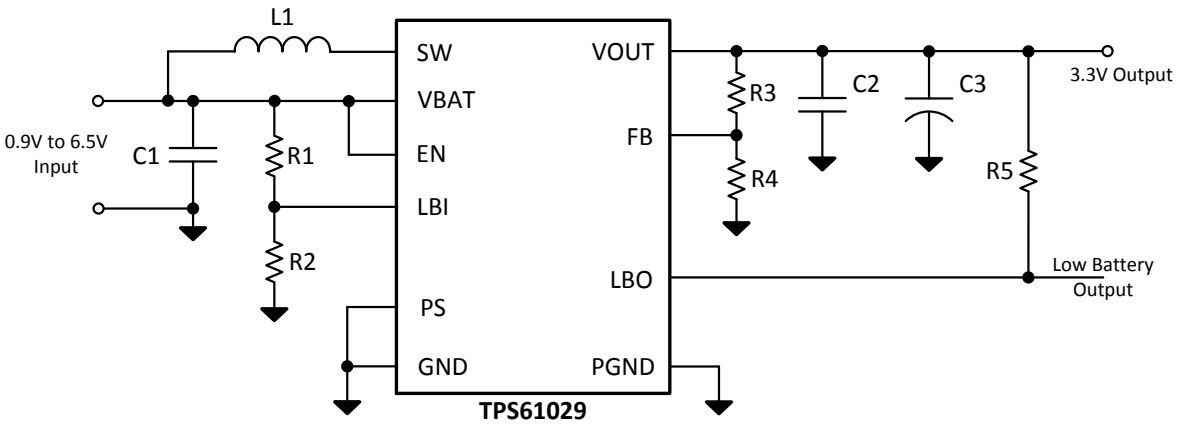

Figure 4: Typical schematic for theTPS61029

3.1.3 MSP430FR5969

The MSP430 ULP FRAM platform combines uniquely embedded FRAM and a holistic ULP system architecture, allowing innovators to increase performance at lowered energy budgets. FRAM technology combines the speed, flexibility, and endurance of SRAM with the stability and reliability of flash with much lower power.

The MSP430 ULP FRAM portfolio consists of a diverse set of devices featuring FRAM, the ULP 16-bit MSP430 CPU, and intelligent peripherals targeted for various applications. The ULP architecture showcases seven low-power modes, optimized to achieve extended battery life in energy-challenged applications. Some of the main features include:

- Embedded Microcontroller
  - 16-Bit RISC Architecture up to 16-MHz Clock
  - Wide Supply Voltage Range: (1.8 V to 3.6 V) (Minimum supply voltage is restricted by SVS levels.)
- Optimized Ultra-Low-Power Modes
  - Active Mode: Approximately 100 µA/MHz
  - Standby (LPM3 With VLO): 0.4 µA (Typical)
  - Real-Time Clock (LPM3.5): 0.25 µA (Typical) (RTC is clocked by a 3.7-pF Crystal.)
  - Shutdown (LPM4.5): 0.02 µA (Typical)
- Ultra-Low-Power Ferroelectric RAM (FRAM)
  - Up to 64KB of Nonvolatile Memory
  - Ultra-Low-Power Writes
  - Fast Write at 125 ns Per Word (64KB in 4 ms)
  - Unified Memory = Program + Data + Storage in One Single Space
  - 10^{15} Write Cycle Endurance
  - Radiation Resistant and Nonmagnetic
- Intelligent Digital Peripherals
  - 32-Bit Hardware Multiplier (MPY)
  - Three-Channel Internal DMA
  - Real-Time Clock (RTC) With Calendar and Alarm Functions
  - Five 16-Bit Timers With up to Seven Capture/Compare Registers Each
  - 16-Bit Cyclic Redundancy Checker (CRC)
- High-Performance Analog
  - 16-Channel Analog Comparator
  - 12-Bit Analog-to-Digital Converter (ADC) With Internal Reference and Sample-and-Hold and up to 16 External Input Channels
- Multifunction Input/Output Ports
  - All Pins Support Capacitive Touch Capability With No Need for External Components
  - Accessible Bit-, Byte-, and Word-Wise (in Pairs)
  - Edge-Selectable Wake From LPM on All Ports
  - Programmable Pullup and Pulldown on All Ports
- Enhanced Serial Communication
  - eUSCI_A0 and eUSCI_A1 Support
    - UART With Automatic Baud-Rate Detection
    - IrDA Encode and Decode
    - SPI at Rates up to 10 Mbps
  - eUSCI_B0 Supports
    - I^2C With Multiple Slave Addressing
    - SPI at Rates up to 8 Mbps
  - Hardware UART and I^2C Bootstrap Loader (BSL)
- Flexible Clock System
  - Fixed-Frequency DCO With 10 Selectable Factory-Trimmed Frequencies
  - Low-Power Low-Frequency Internal Clock Source (VLO)
  - 32-kHz Crystals (LFXT)
  - High-Frequency Crystals (HFXT)

MODE	CONSUMPTION (TYPICAL)
Active Mode	103uA/MHz
Standby (LPM3 with VLO)	0.4uA
Real-time clock (LPM3.5 with crystal)	0.5uA
Shutdown (LPM4.5)	0.02uA

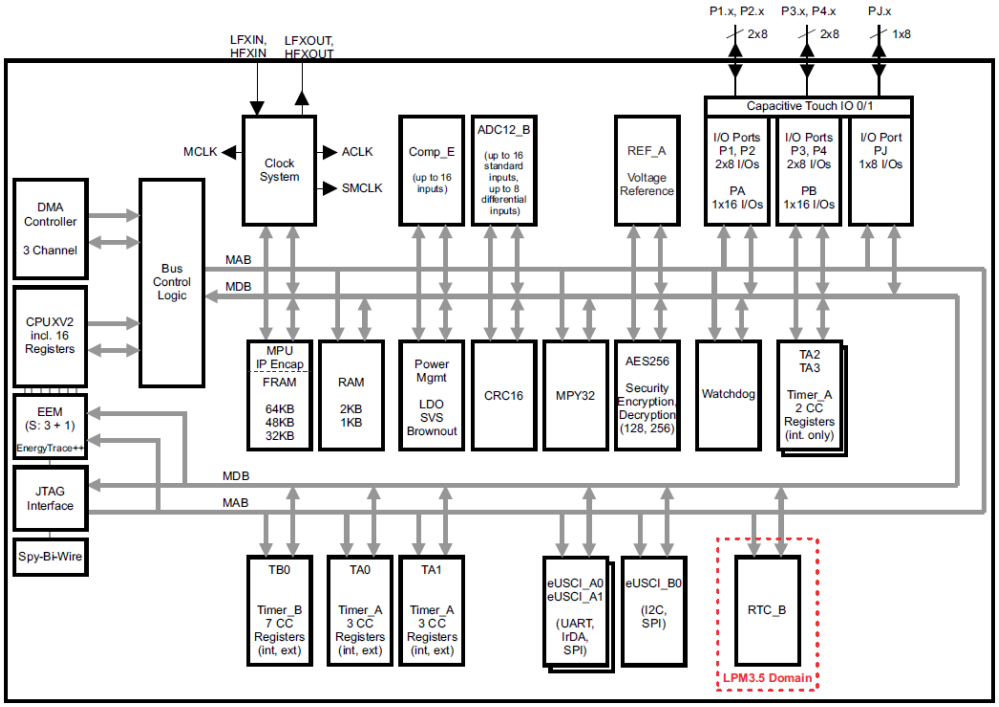

Figure 5: MSP430FR5969 functional block diagram

4 System Design

4.1 Theory

The capacitive sensors used for the proximity sensor and buttons are based on an L-C resonator (tank) circuit. The frequency of the tank is given by the formula:

$$f_{SENSOR} = \frac{1}{2\pi\sqrt{L \cdot (C_{FIXED} + C_{SENSOR})}} \quad (1)$$

The L-C tank that creates the sensor oscillation waveform is a combination of a shielded SMT inductor and capacitance that is made up of a fixed SMT capacitor (C_{FIXED}) on the board, plus a variable capacitor formed by the sensor plate (C_{SENSOR}), relative to ground, as shown in Figure 6. As a hand approaches the sensor, the capacitance to ground varies, causing the frequency of the tank to vary. The FDC2214 measures the change in the oscillation frequency. The fixed SMT capacitor ensures that the LC tank starts up within the sensor frequency specifications since the isolated sensor is relative to GND, not to INxB input.

An important advantage of the LC tank architecture as a capacitive sensor is that it is inherently a narrowband filter and rejects any noise frequencies outside of its band-pass range. It is possible to design the oscillation frequency so that the known noise frequencies do not interfere with the sensor. This is accomplished by selecting appropriate values for L and C. Once the initial component values for the sensor are selected, measurements of the sensor frequency range (with target) should be captured to ensure that the oscillation frequency is between 10 kHz - 10MHz, and that the effective sensor frequency range avoids known noise sources. Iteration on L and C values may be required.

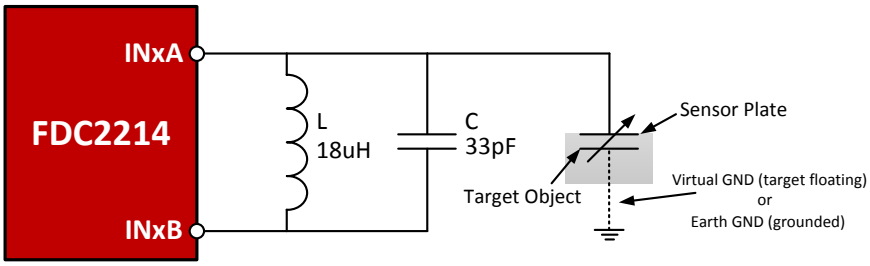

Figure 6: Sensor and L-C tank connection to the FDC2214

4.2 Grounded versus Floating Systems

There are two typical scenarios in how a capacitive sensing system is designed relative to its ground reference: a grounded system and a floating system. A grounded system means the system is referenced to or very close to earth ground. A floating system means the system is referenced to the “ground” reference of the source that is generating the power for the system, for example a battery. As an example, a laptop that is operating with its charger connected to a wall outlet is grounded whereas a laptop powered solely on its battery is a floating system.

The sensitivity of a grounded system is more significant compared to a floating system, especially if the intended target is the human body. The human body will have a voltage potential very close to earth ground (same or very close to system ground) while the voltage potential of the floating system can be significantly different. This difference in potential directly corresponds to a difference in sensitivity or sensing distance.

One system level issue that needs to be taken into consideration is the capacitive coupling through the power and signal lines of a floating system. A very small change in capacitance (on the order of 1fF) is usually required in proximity sensing applications to achieve the maximum sensing distance possible. The power and external signal lines need to be isolated from these capacitive interactions in a floating

system. One example of capacitive coupling interference source includes a USB cable. As the human hand approaches the cable in a grounded system, the change in capacitance is typically less than the detection threshold of the system. For a floating system, the system ground potential can fluctuate as the hand approaches the USB cable. This is seen as a change in capacitance, which may exceed the detections threshold, and cannot be distinguished from a valid event. For this reason***, battery operated systems that employ proximity sensing should have a compact mechanical form such that signal and power cables are not needed***.

Some ways to reduce the effects from capacitive coupling include:

- **Increase threshold parameters** – Increasing the detection threshold will make it less likely that any shift in the measured capacitance magnitude caused by coupling will trigger a detection event.
- **Larger ground plane** – Using a larger local system ground plane increases the amount of parasitic capacitance in the system and can affect sensitivity. The reduction in sensitivity is dependent on the location and position of the ground relative to the sensor.

4.3 Sensor Design

Sensor design is critical for proximity sensing since proximity sensing requires detecting and processing small changes in capacitance from a baseline measurement. For capacitive touch buttons, it's not as critical but there are factors to take into consideration for both proximity and capacitive touch button applications to guarantee designed sensitivity performance in the field. Several factors that affect sensitivity of a sensor are:

- Sensor size area
- System and environment noise
- Size and location of the nearest ground source/plane

4.3.1 Sensor Shape

The shape of the sensor may assume several possible geometries. Some of the most common sensor shapes are shown in Figure 7. The sensitivity of a solid square and circle are comparable due to similar total area. A rectangular sensor has the ability to achieve higher sensing range in applications with specific physical constraints. For example, if the sensor width is 0.5cm and the length is 40cm, fringing effects lengthwise will play a role in increased sensitivity relative to the position of the sensor to the target object. In many cases, the bezel sensor offers flexibility in the layout of the electronics since a square area on the board does not have to be reserved for the sensor.

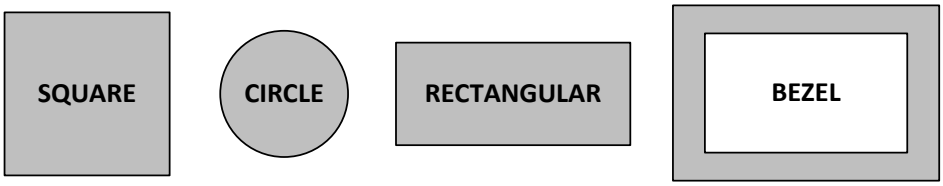

Figure 7: Common sensor shape configurations

It is a straightforward process to compare the sensing distance of solid continuous sensors, but comparing solid sensors to bezel shaped sensors is more complex because the even charge distribution is spatially distributed over a wider area. A sensitivity analysis was performed to verify and compare the sensing distance between the bezel and solid configuration of the same total sensor area. Three sensors of different dimensions were created to have the same total sensor area of $50cm^2$:

- Sensor1 - 7.1cm x 7.1cm solid square sensor
- Sensor2 - 12cm x 10cm bezel sensor with a 1.3cm width
- Sensor3 - 17cm x 16cm bezel sensor with a 0.8cm width

Table 2 shows all three sensors have similar sensing distances regardless of effective spatial area that the area of the sensors covers. With this test setup, sensing distance is ultimately dictated by total sensor area and is independent of the geometry of the sensor.

Table 2: Sensitivity comparison between solid and bezel shaped sensors

Sensor	Total Area Size (cm^2)	Effective Spatial Area (cm^2)	Max Sensing Distance (cm)
1	50.41	50.41	48-49
2	50.44	120	48-50
3	50.24	272	48-50

The data shown in Table 2 were based on a grounded system configuration using the same algorithm and threshold parameters. For more information on sensor design for proximity sensing applications, refer to the application note Capacitive Proximity Sensing using the FDC2x1y (SNOA940).

4.3.2 Proximity Sensor

The proximity sensor on the board was designed to detect a human hand at 50cm using a grounded system and 10cm with a floating system. Sensitivity is defined as maximum sensing distance, at which point the shift in the measured capacitance exceeds the detection threshold, which is determined by the system noise level. Figure 8 shows a plot of the sensing distance the FDC2214 can achieve with a given sensor size area in a grounded system. A solid square sensor was used to collect the data in Figure 8.

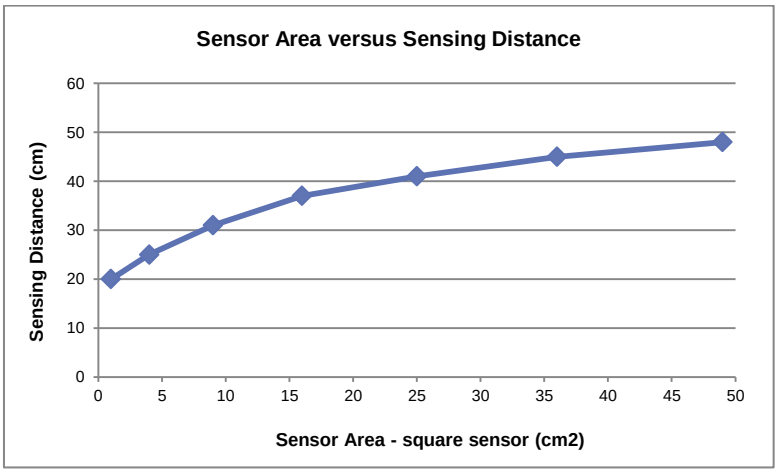

Figure 8: FDC2214 sensor size area versus sensing distance

The proximity sensor on the board is arranged around the edges of the board in a bezel configuration. The actual sensor size area is $59cm^2$ with the spatial sensor size area spanning $121cm^2$. All of the electronics are located in the middle of the proximity sensor.

One of the major factors that affect sensitivity of a proximity sensor is the size and location of the nearest ground potential. The layout of the board minimizes the ground plane as much as possible. A ground plane underneath the sensor will significantly reduce sensitivity. For example, if a ground shield is directly below and the same size as the sensor, sensitivity will be reduced by 50%. Noise in the system and in the environment will also affect sensing performance. Plenty of noise margin needs to be built into the data processing to allow variations in the system environment.

4.3.3 Capacitive Touch Buttons

The circular buttons measure 20.32mm (0.8 inches) in diameter. Capacitive touch buttons require less attention to sensitivity in terms detecting very small changes in capacitance simply because the intent is to detect a touch event. Typically, changes in capacitance on the order of picofarads are required in detecting button presses. The same factors that affect sensitivity for proximity still apply for capacitive touch buttons. A solid or hatched ground pad/shield underneath the button sensor can be used to moderate the sensitivity of the button and mitigate unintentional touch events.

In most applications, the user interacts with the button sensor directly. In some applications there may be a protective cover or a piece of isolation material to prevent direct contact with the sensor (for quality and reliability purposes). Sensitivity performance is dependent on the material and thickness of the material. Figure 9 shows a simulated sensitivity analysis for a proximity sensor. Capacitive touch buttons rely on a very large response to determine when a press is detected directly on the sensor. The simulation shows that at close range, including the touch condition, a protective cover (in this case PVC) can actually enhance the response. However, this effect is observed over a limited range and at longer ranges shows very little impact.

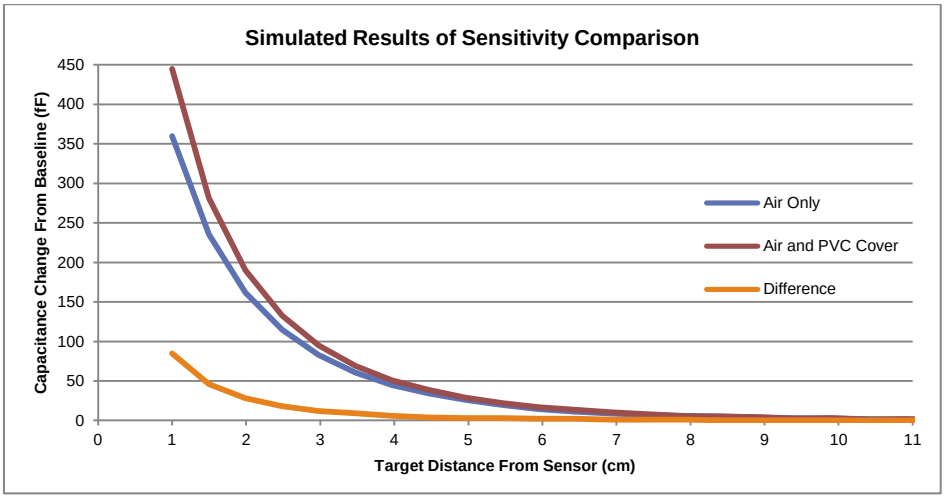

Figure 9. Comparison of Capacitance vs target position for covered and non-covered sensors

5 Hardware

Figure 10 illustrates the features of the top side and bottom side of the board. The proximity sensor consists of a copper bezel arranged around the perimeter of the board. The board is 10.16cm by 12.7cm (4x5 inches). The proximity sensor is 19.05mm (0.75 inches) wide and conforms to the edges of the board. The buttons are 20.32mm (0.8 inches) diameter sensors arranged in the center of the board. A cut out on the proximity sensor where the battery is located is necessary since the battery acts as a ground. This limits the amount of direct capacitive coupling seen by the sensor.

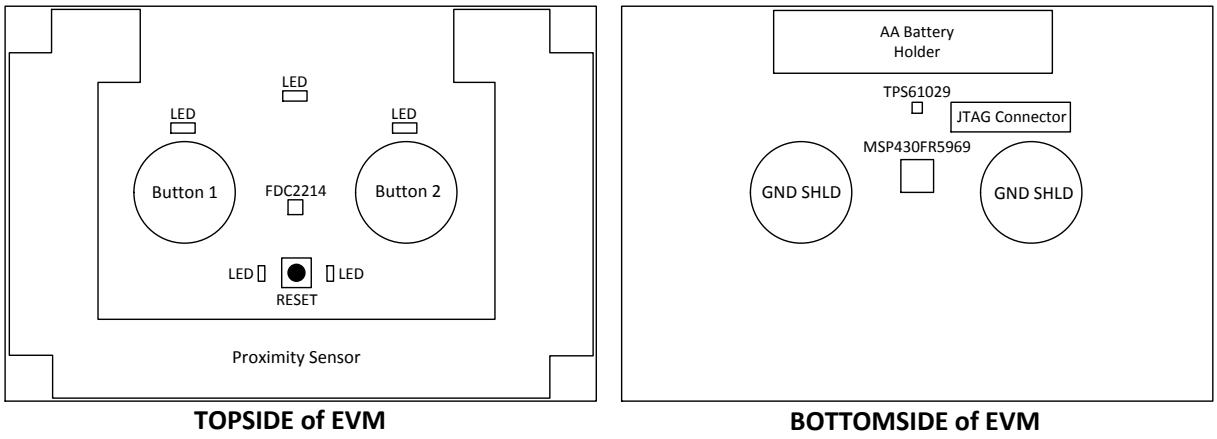

Figure 10: Component layout location of board on top side and bottom side

5.1 Reset Button

A reset button (Figure 10) is included in the design to perform a soft reset to the system if there are any disruptions to the board relative to its environment. For example, if the board is picked up and moved to a different area, its baseline capacitance can dramatically change. The derivative-integration algorithm implemented in this system may take some time to recover from this change in the baseline capacitance, so the reset button can be used to eliminate this recovery time. Once the reset button is pressed, LED D2 and D3 near the button will temporarily light up indicating that an initial calibration is being performed.

> **NOTE:** A two second delay is implemented prior to the calibration process. During calibration, no target or object should be in the intended sensing area. The LEDs will turn off after calibration and the system will be fully operational.

5.2 Optional Features Descriptions

There are several optional features (Table 3) implemented in the design that can be suitable for future system investigations:

Table 3: Optional feature use cases

Part Designator	Description	Use Case
J2	3 GPIO pinouts on a 3 pin 100mil header	Debug and prototype
R24	Pull-up resistor on the supply pin of the FDC2214	Allows for current measurements for low power (LP) applications
R25	Pull-up resistor on the supply pin of the external oscillator	Power gating to reduce current for LP applications
R26	Pull-down resistor on the enable pin of the external oscillator	Enable gating to reduce current consumption for LP applications
R28, R29, R31	Series resistors on channel inputs of FDC2214 to sensors	Connecting external sensors for evaluation and prototyping purposes

R32, R34	Resistors to connect GND SHLD capabilities	Understanding how ground shields affect sensitivity and interference

5.3 FDC2214 Register Configuration

The full set of register contents used to configure the FDC2214 for this application can be found in Table 4.

Table 4: FDC2214 register configuration

Register Address	Name	Value	Description
0x08	RCOUNT_CH0	0x9C40	RCOUNT of 40000 (~16ms conversion time)
0x09	RCOUNT_CH1	0x03E8	RCOUNT of 1000 (~400us conversion time)
0x0A	RCOUNT_CH2	0x03E8	RCOUNT of 1000 (~400us conversion time)
0x10	SETTLECOUNT_CH0	0x0064	100 cycles before measurement taken
0x11	SETTLECOUNT_CH1	0x0064	100 cycles before measurement taken
0x12	SETTLECOUNT_CH2	0x0064	100 cycles before measurement taken
0x19	ERROR_CONFIG	0x0001	Report data ready flag by asserting INTB pin
0x1A	CONFIG	0x1E01	Active mode enabled Low power activation mode enabled Reference frequency provided from CLKIN pin INTB pin enabled Normal sensor drive current enabled
0x1B	MUX_CONFIG	0xA20D	Auto-scan conversions enabled Auto-scan sequence: Ch0, Ch1, CH2 Deglitch filter: 10MHz
0x1E	DRIVE_CURRENT_CH0	0x5000	Current drive set to 0.069mA
0x1F	DRIVE_CURRENT_CH1	0x5800	Current drive set to 0.081mA
0x20	DRIVE_CURRENT_CH2	0x5800	Current drive set to 0.081mA

5.4 Additional Debugging Features

There are several hooks integrated in the design to debug the power supply rails and the I^2C bus lines. To debug the system in real time, the backchannel UART on the MSP-FET tool is connected to the UART_A1 module on the MSP430FR5969. The JTAG connector pins 12 and 14 (blue colored pins in Figure 11) correspond to the transmit and receive signal lines respectively. The firmware implements functions to transmit ASCII characters to a PC serial COM port host. The backchannel UART is disabled (relevant code is commented out) in the firmware by default. To enable the UART functions, uncomment the UART code, recompile the firmware, and load it to the MSP430 to use this functionality.

6 Firmware Programming

Programming new firmware on to the MSP430 through Code Composer Studio (CCS) can be performed in two ways:

- MSP-FET emulation tool via JTAG connector
- Spy-by-wire from an MSP430 LaunchPad

The JTAG connector (as shown in Figure 11) can be used with the MSP-FET tool for programming. Table 5 shows the signal names assigned to the pins of the JTAG connector. The JTAG is not populated by default so the connector or 100mil pitched headers need to be soldered on to the board to use for programming and debugging.

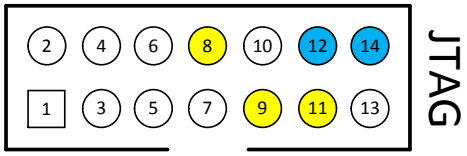

Figure 11: JTAG pin out diagram

Table 5: JTAG connector pin assignment

Pin	Signal	Description
1	TDO	JTAG data output
2	VCC_TOOL	JTAG voltage selection from tool
3	TDI	JTAG data input and TCLK input
4	VCC_TARGET	Not connected
5	TMS	Signal to control the JTAG state machine
6	NC	Not connected
7	TCK	JTAG clock input
8	SBWTCK	Spy-by-wire clock
9	GND	Ground
10	NC	Not connected
11	SBWTDIO	Spy-by-wire bidirectional signal IO
12	A1_TX	UART_A1 transmit signal (for debugging)
13	NC	Not Connected
14	A1_RX	UART_A1 receive signal (for debugging)

For Spy-By-Wire (SBW) interface programming, Figure 11 indicates the yellow colored pins 8, 9, and 11 (SBWTCK, GND, and SBWTDIO) that need to be connected to the isolation block connections on the MSP430 LaunchPad. SBWRST and SBWTST pins on the LaunchPad need to be connected to SBWTDIO and SBWTCK test points, respectively. A common ground is required between the board and LaunchPad for proper operation.

7 Data Processing

7.1 Derivative-Integration Algorithm

A derivative-integration algorithm (pseudo code shown in Figure 12) is used to process the data to determine whether a target object was detected or not. It is used to process data for both the proximity sensor and capacitive touch buttons; the only difference between the two would be the derivative and integration thresholds for each sensor to obtain a robust and highly sensitive response. Note that the algorithm operates on raw code values, not capacitance values. As a hand approaches the sensor, the system capacitance increases, which results in a corresponding decrease in the raw output code values.

The algorithm works tracking the rate of change or derivative (D[i]) between the current measurement (X[i]) and previous measurement (X[i-1]). If the derivative threshold (DT) is exceeded, an integral accumulation is updated. This integral value is tested against a threshold (IT) and a detection decision is made. Proximity sensing applications require the detection of small capacitance changes (on the order of fF). This requires the derivative threshold (DT) to be very low. Changes in capacitance due to noise can be a severe problem, especially if the DT is too low. The integral of the derivative (I[i]) can start to accumulate and falsely trigger as a detection. Random noise will stabilize the integral value so that the mean is zero (no capacitance drift occurs). Setting a slightly high integration threshold (IT) can allow enough noise margin for non-random noise.

As an example, once the human hand approaches the sensing area of the board, the integration value will start to accumulate as along as the derivative of the measurements hit the derivative threshold. If the hand has been “detected” by the device (integral value goes below IT) and stops in the sensing area, the derivative flattens out and the integral stops accumulating. As the hand moves away from the sensor, the integral recedes until it goes above the threshold. This indicates the target object is outside of the intended sensing range of the board.

```
X[i-1] = X[0]
I[i-1] = 0

Loop1:
D[i] = X[i] - X[i-1]
Is (ABS(D[i]) greater than DT)?
        true:
                I[i] = I[i-1] + D[i]
        else:
                I[i] = I[i-1]
Is (-I[i] ≥ IT)
        true:
                Object detected
                I[i-1] = I[i]
        else:
                Object not detected
                I[i-1] = I[i]*L
```

Parameters
IT = Integration threshold
DT = Derivative threshold
L = Leakage factor
X[i] = Current sample point
X[i-1] = Previous sample point
D[i] = Derivative
I[i] = Integral of derivative
I[i-1] = Previous integral of derivative

Figure 12: Pseudo code for the derivative-integration algorithm

The leakage factor (L) is applied to the integral and is a value between 0 (instant dissipation) and 1 (no dissipation). It is typically set at 0.99 to represent that the algorithm has some memory and information on past values to determine where the detection boundary occurs. Various leakage factors can be used for a faster recovery time if the integral swings too far positive. This will cause temporary sensitivity reduction until the integral can stabilize near zero.

For capacitive touch button applications, a higher derivative threshold is typically used. The integration threshold can be optimized based on the desired button response. Multiple derivative and integration thresholds can be implemented to filter out any high frequency noise seen in the sampled measurements and increase the sensitivity response.

Figure 13 shows an example of the FDC2214 raw code waveform with a target in proximity to the sensor. Figure 14 corresponds to the derivative of the raw code and Figure 15 corresponds to the integral count. As the derivative becomes more negative (object approaching closer to the proximity sensor), the integral count matches the raw code signal as expected.

The threshold can also be optimized to be robust against any slow moving drift that occurs. Figure 16 shows how a drift in the raw code is compensated in the integral count. The signal is preserved without any distortions due to the slow upward drift.

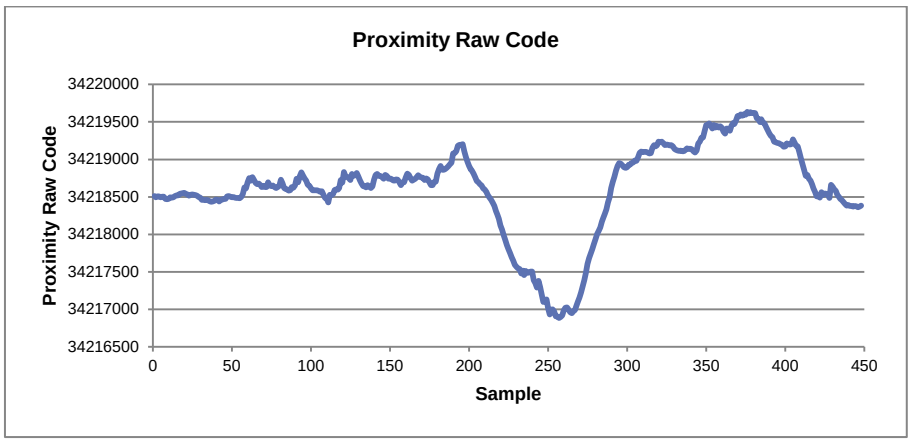

Figure 13: Proximity raw code example 1

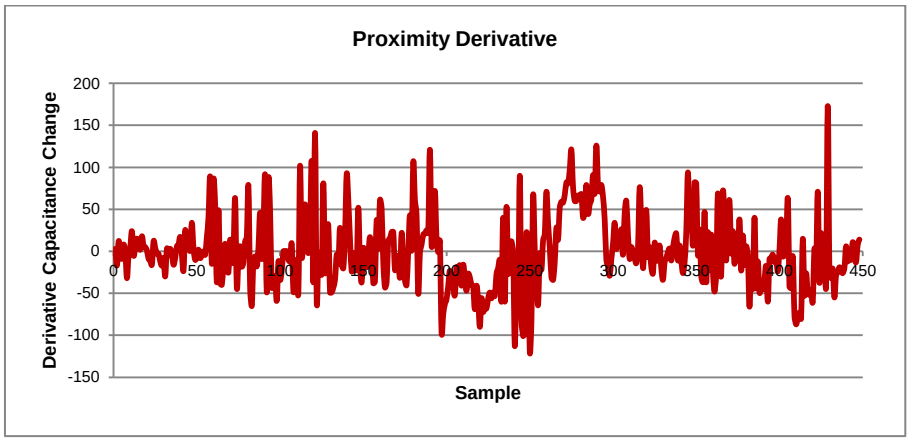

Figure 14: Proximity derivative example 1

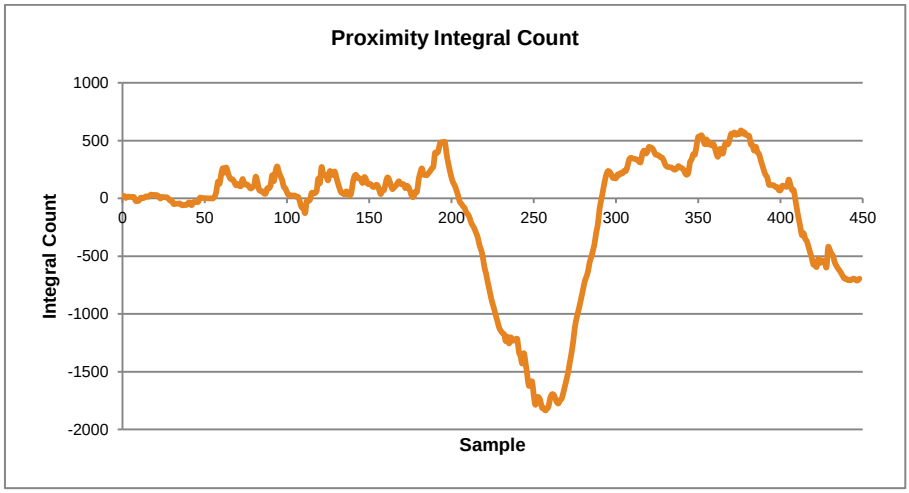

Figure 15: Proximity integral count example 1

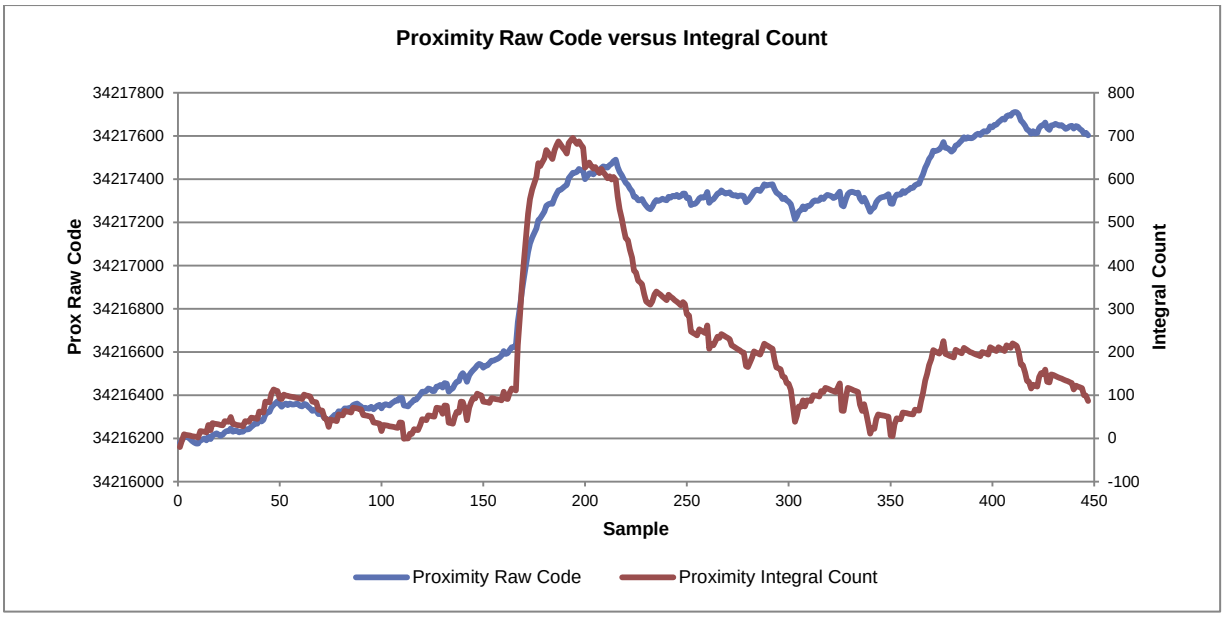

Figure 16: Proximity raw code versus integral count example

7.2 IIR Filter Implementation

To improve the signal-to-noise ratio in the measurements, an IIR filter was implemented to process the data and obtain a smooth measurement prior to sending it through the derivative-integration algorithm. The IIR filter implementation is similar to a moving average except that previous values do not have to be stored and shifted out of the summing order. This process saves memory and computational time at the expense of slight accuracy degradation.

Making N a power of two allows bit shifting instead of actual division and multiplication, thus saving computational cycles and simplifying the MCU code. The following equation illustrates the filter computation. The current raw sample value is val[i]. The output result, Avg[i], is the input to the derivative-integral algorithm, represented by X[i] in Figure 12.

$$Avg[i] = \frac{(Avg[i-1] \times N) - Avg[i-1] + val[i]}{N} \quad (2)$$

8 Test Data

The testing environment conditions play a significant role in sensitivity and noise in the system. Testing reported here was performed in an area where the impact of external interference and nearby grounded planes was minimized. This section provides basic data on the operation and sensitivity performance of the proximity sensor and capacitive touch buttons.

8.1 Basic Sensor Operation

Table 6 shows the signal properties of the proximity sensor and one of the capacitive touch buttons. They were obtained by probing either INA or INB of each channel with an oscilloscope. Figure 17 through Figure 19 illustrate the waveforms for the proximity sensor and the capacitive touch buttons. The recommended voltage amplitude for the oscillation waveform is between 1.2 and 1.8 V_{pp}. Anything over 1.8 V_{pp} is not recommended because the ESD clamps will turn on and become part of the L-C tank, causing a frequency shift. The voltage amplitude is controlled by setting the current drive value for the channel. The sensor will still function for voltage amplitudes to a minimum of 0.4 V_{pp}, but the SNR will degrade. More information on the impacts of adjusting drive current strength and how to configure it can be found in Section 8.3.

The oscilloscope probe will have a capacitive loading effect when probing the sensor signal lines. A FET probe with low capacitance should be used to minimize the effects.

Table 6: Proximity and capacitive touch sensor properties

	Proximity Sensor	Capacitive Touch Button 1	Capacitive Touch Button 2
Sensor Frequency	5.30	5.41	5.60
Amplitude (mV)	1.22	1.44	1.42
Settling Time (us)	3.89	3.33	3.15
Current Drive Setting (mA)	0.069	0.081	0.081

Figure 17 and Figure 18 show the oscillation and startup waveforms for the proximity sensor and capacitive touch buttons. The yellow waveform corresponds to the proximity sensor while the green and magenta waveform corresponds to the capacitive touch button 1 and 2. The FDC2214 may be configured for current overdrive at the beginning of a conversion cycle, as illustrated in Figure 18. This feature can be used to reduce the startup up time of the oscillation and hence shorten the overall conversion time.

Figure 19 shows the multiplexing operation of the FDC2214 to collect the measurements from the various sensors. The proximity sensor's measurements (yellow) are significantly longer than the capacitive touch buttons measurements (green and magenta) to obtain a better signal-to-noise ratio. There is a tradeoff between sampling rate and resolution. For example, the higher the sampling rate, the lower the resolution. Proximity sensing applications require a high resolution to detect small changes in capacitance (on the order of a few femtofarads) from the baseline value (no target present). Capacitive touch buttons requirements are the opposite, in which high resolution is not necessary for a change in capacitance on the order of picofarads. The proximity sensor has a conversion time of approximately 16ms while the capacitive touch buttons have a conversion time of approximately 400us.

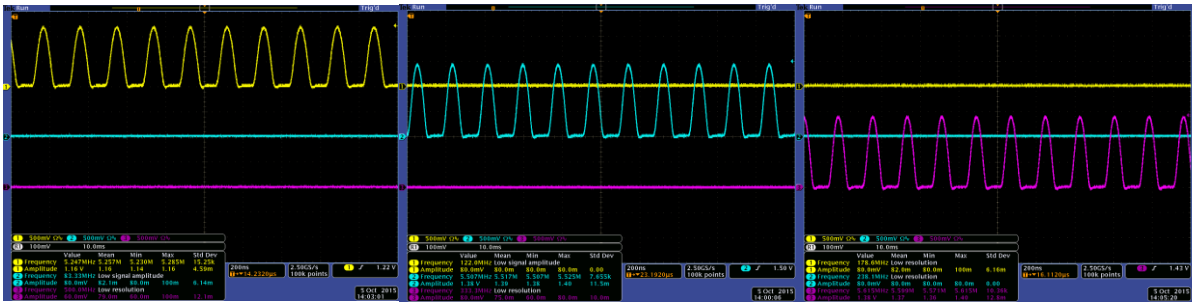

Figure 17: Proximity sensor waveform (yellow), cap touch button 1/2 waveforms (green and magenta)

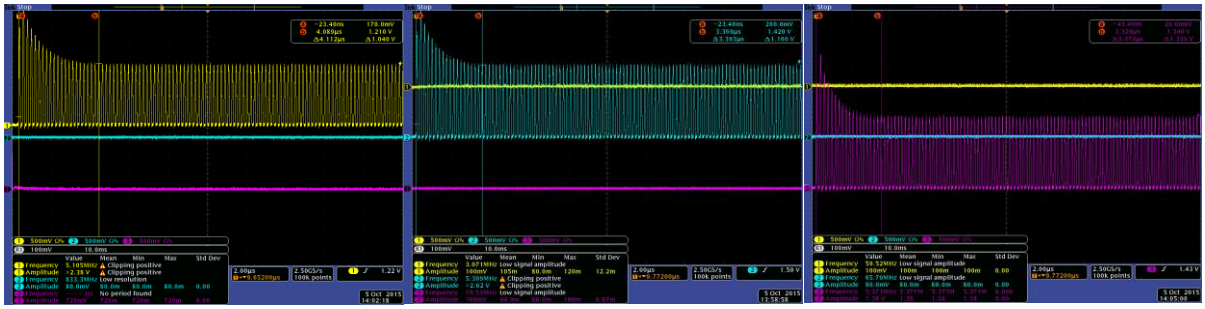

Figure 18: Proximity startup waveform (yellow), cap touch button 1/2 startup waveforms (green, magenta)

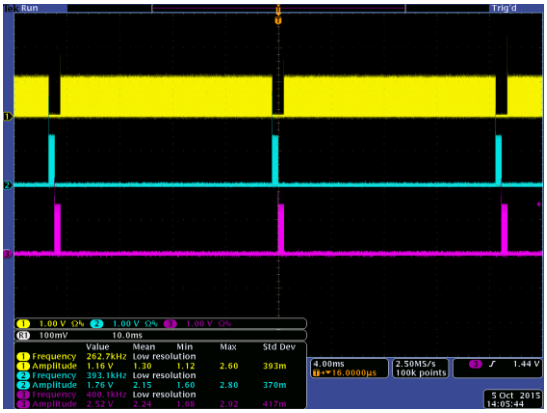

Figure 19: Sensor multiplexing – proximity (yellow), cap touch button 1 & 2 (green, magenta)

8.2 Sensitivity Analysis

The board was designed with a bezel shaped sensor that surrounds the edges of the board. The firmware and derivative-integration algorithm used to process the raw data was optimized to get the maximum sensing distance possible. The board achieves a maximum sensing distance of 10cm (4 inches) as a floating system and 50cm as a grounded system. The cap touch buttons are optimized to response quickly to rapid button presses.

In many applications, the sensor may not be directly exposed. It may be covered with a particular material and located some distance away from it. A sensitivity analysis was performed with two types of materials of different thicknesses and spacing distances from the proximity sensor to determine the sensing behavior through these materials. Figure 20 shows the two types of covers (acrylic and PVC) that were used for this analysis. The middle sections were cut out to accommodate the SMT parts and through hole pads that are located on the topside of the board.

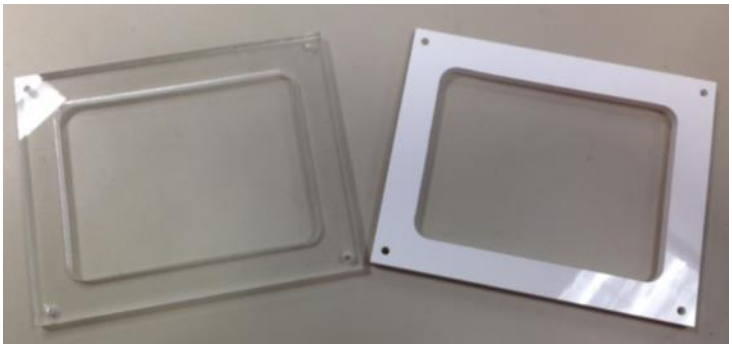

Figure 20: Acrylic and PVC covers

8.2.1 Theory and Simulation Results

Theory suggests from the parallel plate formula that inserting a material with a larger dielectric constant than air between the two plates will result in a larger capacitance change. The change in capacitance from the material is much larger than that of air. Increased sensitivity is not noticeable at farther distances, but becomes more prominent as the two plates are much closer since the air thickness is reduced with the material between the plates. This concept can be applied to the proximity sensing case with an isolated sensor. Simulations were performed to verify this concept with typical proximity sensing applications.

A 2D finite element analysis modeling program (FEMM) was used to setup the planar models and obtain the capacitance value trend as the target (a human hand) approaches the sensor. The model consisted of a 5x5cm sensor, a 2x5cm GND source located 5cm away from the sensor, and a 15cm wide human target. One simulation was performed with no cover and then compared with another simulation with a 6.35cm (1/4inch) thick PVC cover. This simulation does not fully represent the absolute system performance because it is impossible to accurately model the more complex real world environment. Its main purpose was to verify the relationship between increased sensitivity with a larger dielectric material located on the sensor. The sensitivity comparison with and without a PVC cover are shown in Figure 21. As theory suggested, the sensitivity increases slightly when a cover material is directly over the sensor. The green line shows the difference between the two simulation plots. The air gap is minimized and sensitivity is enhanced especially at closer target distances. For larger distances, the differential change in capacitance is not as pronounced, but the sensing distance can still be slightly improved. Because proximity sensing applications require detection of small changes in capacitance, even a capacitance increase of 10-20fF near the maximum sensing distance translates to a noticeable amount.

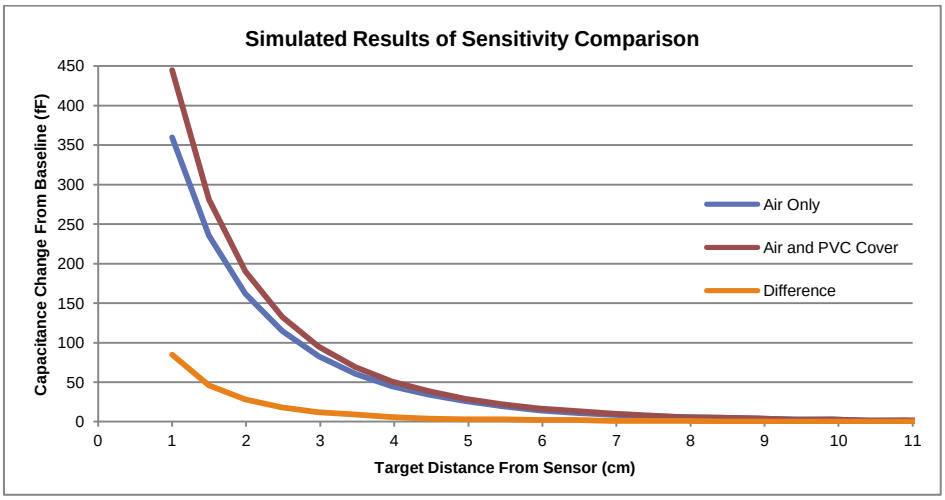

Figure 21: Simulated results of sensitivity comparison

Table 7 shows the sensitivity comparison between no cover, an acrylic cover, and a PVC cover of various thicknesses, using the floating system. The covers are flush with the sensor to minimize the air gap. The maximum sensing range obtained for the board by itself was 10-11cm. As predicted by theory and simulations, sensitivity does increase by having a material with larger dielectric constant than air (dielectric constant ~1) placed next to the sensor. As the thickness of the material increases, sensitivity increases slightly by 1-2cm. The results for acrylic and PVC are fairly similar since their dielectric constants are similar (~3).

Table 7: Sensitivity analysis comparison - flush to the sensor (floating system)

	Thickness		Maximum Sensing Range	
	in	mm	cm	in
Uncovered			10-11	3.9-4.3
Acrylic	1/8	3.175	10-11	3.9-4.3
	1/4	6.35	11-12	4.3-4.7
	1/2	12.7	11-12	4.3-4.7
PVC	1/8	3.175	10-11	3.9-4.3
	1/4	6.35	10-11	3.9-4.3

Since a floating system is not as sensitive when compared to a grounded system, having a cover on top of the sensor does not have a noticeable effect on the maximum sensing range that can be achieved. It is much more noticeable in a grounded system. Table 8 shows a grounded system with a cover flush on top of the sensor. The maximum sensing distance increases by a few centimeters as the thickness of the material increases.

Table 8: Sensitivity analysis comparison - flush to the sensor (grounded system)

	Thickness		Maximum Sensing Range	
	in	mm	cm	in
Uncovered			45-48	17.7-18.9
Acrylic	1/8	3.175	47-49	18.5-19.3
	1/4	6.35	49-50	19.3-19.7
	1/2	12.7	50-52	19.7-20.4
	3/4	19.05	51-53	20-20.9
PVC	1/8	3.175	46-48	18.1-18.9
	1/4	6.35	47-50	18.5-19.7

Table 9 shows the sensitivity comparison with the same materials as above but spaced at various distances from the sensor. As the gap between the sensor and the material increases, the sensing distance decreases regardless of the thickness of the material. It is not noticeable for a floating system but evident in a grounded system. Compared to the experimental results in Table 7, the system is most sensitive and achieves the largest sensing distance when the air gap between the sensor and material is minimized. Since the change in capacitance decreases exponentially with distance to target, the sensing range results in Table 9 are lower than the results in Table 7 due to the air gap (lower dielectric constant). However, ***these test results show that if a cover material with dielectric constant higher than air is used, it is possible to slightly improve sensitivity regardless of the spacing between sensor and the cover.***

Table 9: Sensitivity analysis with various spacing

Material	Spacing between Sensor and Cover		FLOATING SYSTEM		GROUNDED SYSTEM	
			Maximum Sensing Range			
	in	mm	cm	in	cm	in
Uncovered			10-12	3.9 - 4.3	45-48	17.7 - 18.9
1/8" Acrylic	1/8	3.175	10-11	3.9 - 4.3	48-50	18.9 - 19.7
	1/4	6.35	10-11	3.9 - 4.3	46-49	18.1 - 19.3
	1/2	12.7	10-11	3.9 - 4.3	45-47	17.7 - 18.5
1/4" Acrylic	1/8	3.175	9-11	3.5 - 4.3	48-50	18.9 - 19.7
	1/4	6.35	9-10	3.5 - 3.9	46-48	18.1 - 18.9
	1/2	12.7	9-10	3.5 - 3.9	45-47	17.7 - 18.5
1/2" Acrylic	1/8	3.175	9-11	3.5 - 4.3	47-50	18.5 - 19.7
	1/4	6.35	9-11	3.5 - 4.3	46-48	18.1 - 18.9

8.3 Sensitivity vs EMI Emissions

Proximity sensing applications require the system to be optimized to reach the maximum sensing distance possible for a given sensor area. Sensor size area, system/environment noise, and size/location of the nearest ground potential all affect sensitivity, but current drive strength (I_{DRIVE}) of the FDC2214 can impact results. The amount of I_{DRIVE} necessary for the LC tank directly corresponds to the voltage amplitude of the waveform and the parasitic resistance losses in the system. The formula below shows the correlations current drive strength to voltage amplitude.

$$V_{SENSOR} = I_{DRIVE} \times R_P \quad (3)$$

Where R_P = Parallel resonant resistance of the L-C tank sensor.

The R_P of the sensor is proportional to: $\frac{1}{\sqrt{C_{SENSOR} + C_{FIXED}}}$. C_{FIXED} includes both the fixed capacitance set by the on-board capacitor (33 pF for this reference design) and any constant parasitic capacitance of the board. Because these are typically much greater than the capacitance change caused by a target (typically only a few pF), the change in R_P due to the target is negligible. The appropriate current drive setting is typically determined by measuring the INA or INB channel inputs on an oscilloscope to determine V_{sensor}. An estimated drive current can be determined if the sensor and L-C tank are characterized by an impedance analyzer. If an impedance analyzer is not available, the current drive can adjusted until the appropriate amplitude is obtained. The recommended voltage amplitude for the oscillation waveform is between 1.2-1.8 V_{pp}. Anything over 1.8V_{pp} is not recommended because the ESD clamps will turn on and could cause damage to the device. It is possible to have a voltage amplitude less than 1.2V_{pp} (down to a minimum of 0.4 V_{pp}), but SNR, and therefore sensitivity will degrade.

Each channel of the FDC2214 can be configured with its own I_{DRIVE} setting. Address register 0x1E through 0x21 corresponds to channel 0 to channel 3 respectively. At startup, I_{DRIVE} is default at the lowest current drive setting, 0.016mA. One of 32 different current settings can be selected to optimize the sensitivity of the system. Refer to the FDC2214 datasheet (SNOSCZ5A) for more information on current drive selection.

There is a tradeoff between sensitivity of the system and EMI emissions. By increasing the current drive, the voltage amplitude of the oscillation waveform increases proportionally. Higher voltage amplitude and higher oscillation frequency means a faster slew rate. The FDC2214 by design counts the number of zero crossings to determine the amount of change in oscillation frequency. A faster slew rate reduces the error from jitter during zero crossing counts and results in better resolution and sensitivity. Unfortunately due to increased voltage/current drive, EMI emissions of a half wave rectified sine wave increases since the sensor acts as an antenna. Depending on the application, a balance between sensitivity and EMI emissions may be necessary.

9 Design Files

9.1 Schematics

To download the Schematics for each board, see the design files at TIDA-00466

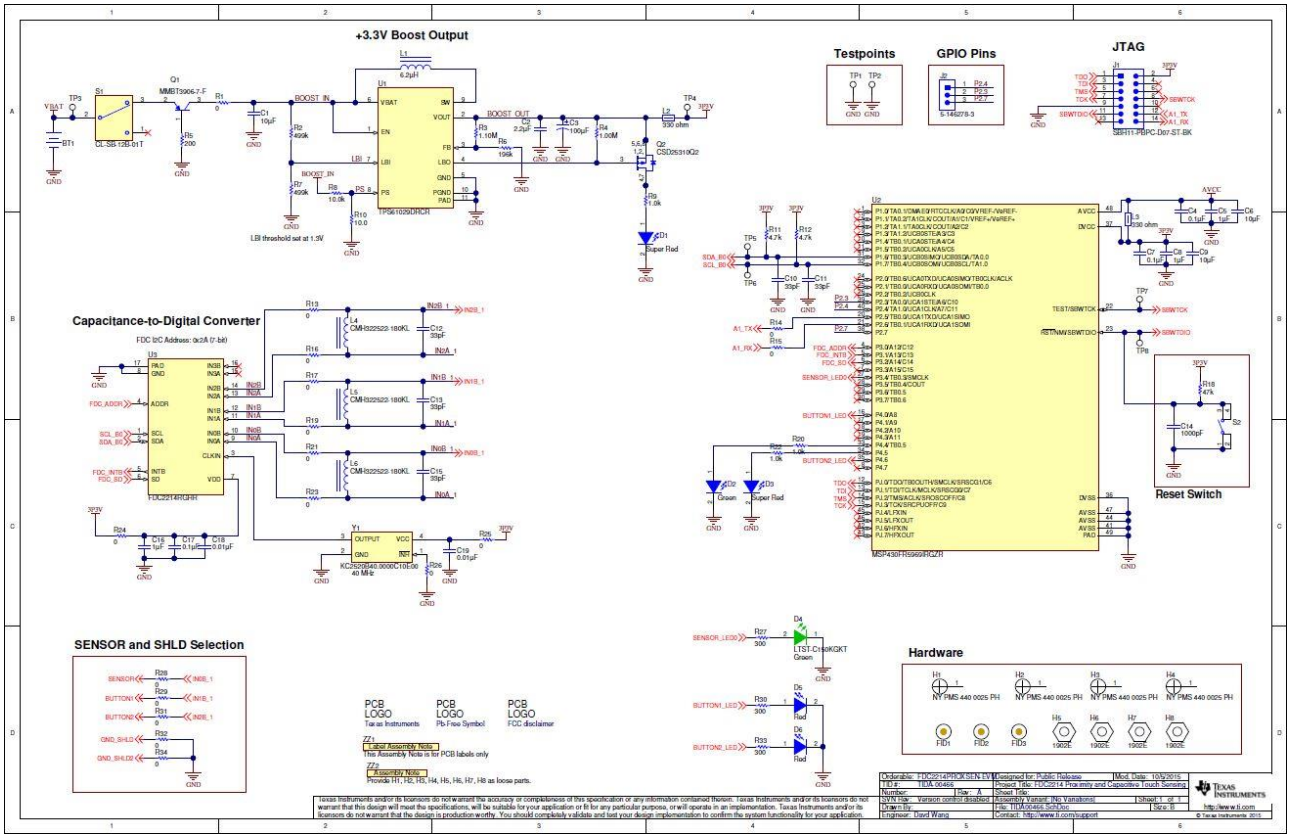

Figure 22: Schematic

9.2 Bill of Materials

To download the Bill of Materials (BOM), see the design files at TIDA-00466.

Table 10: BOM

Designator	Quantity	Value	Description	Package Reference	Part Number	Manufacturer
BT1	1		AA Battery Holder, Through-hole mount		1015	Keystone
C1	1	10µF	CAP, CERM, 10 µF, 6.3 V, +/- 20%, X5R, 0603	0603	GRM188R60J106ME47D	MuRata
C2	1	2.2µF	CAP, CERM, 2.2 µF, 16 V, +/- 10%, X7R, 0805	0805	GRM21BR71C225KA12L	MuRata
C3	1	100µF	CAP, TA, 100 µF, 10 V, +/- 10%, 0.1 ohm, SMD		TPSC107K010R0100	AVX
C4, C7	2	0.1µF	CAP, CERM, 0.1 µF, 16 V, +/- 10%, X7R, 0402	0402	GRM155R71C104KA88D	MuRata
C5, C8	2	1µF	CAP, CERM, 1 µF, 16 V, +/- 10%, X7R, 0603	0603	GRM188R71C105KA12D	MuRata
C6, C9	2	10µF	CAP, CERM, 10 µF, 16 V, +/- 20%, X7R, 0805	0805	EMK212BB7106MG-T	Taiyo Yuden
C10, C11	0	33pF	CAP, CERM, 33 pF, 50 V, +/- 5%, C0G/NP0, 0603	0603	GRM1885C1H330JA01D	MuRata
C12, C13, C15	3	33pF	CAP, CERM, 33 pF, 100 V, +/- 5%, C0G/NP0, 0603	0603	GRM1885C2A330JA01D	MuRata
C14	1	1000pF	CAP, CERM, 1000 pF, 16 V, +/- 10%, X7R, 0603	0603	GRM188R71C102KA01D	MuRata
C16	1	1µF	CAP, CERM, 1 µF, 10 V, +/- 10%, X5R, 0402	0402	GRM155R61A105KE15D	MuRata
C17	1	0.1µF	CAP, CERM, 0.1 µF, 10 V, +/- 10%, X7R, 0402	0402	GRM155R71A104KA01D	MuRata
C18	1	0.01µF	CAP, CERM, 0.01 µF, 16 V, +/- 10%, X7R, 0402	0402	GRM155R71C103KA01D	MuRata
C19	1	0.01µF	CAP, CERM, 0.01 µF, 25 V, +/- 5%, C0G/NP0, 0603	0603	C1608C0G1E103J	TDK

D1, D3	2		LED, Super Red, SMD		SML-LX0603SRW-TR	Lumex
D2	1		LED, Green, SMD		LG L29K-G2J1-24-Z	OSRAM
D4	1		LED, Green, SMD		LTST-C150KGKT	LiteOn
D5, D6	2		LED, Red, SMD		LTST-C170KRKT	Lite-On
FID1, FID2, FID3	0		Fiducial mark. There is nothing to buy or mount.		N/A	N/A
H1, H2, H3, H4	4		Machine Screw, Round, #4-40 x 1/4, Nylon, Philips panhead		NY PMS 440 0025 PH	B&F Fastener Supply
H5, H6, H7, H8	4		Standoff, Hex, 1"L #4-40 Nylon		1902E	Keystone
J1	0		Header (shrouded), 100 mil, 7x2, Gold, TH		SBH11-PBPC-D07-ST-BK	Sullins Connector Solutions
J2	0		Header, 100mil, 3x1, Tin, TH		5-146278-3	TE Connectivity
L1	1	6.2µH	Inductor, Shielded Drum Core, Ferrite, 6.2 µH, 1.8 A, 0.045 ohm, SMD		CDRH5D28NP-6R2NC	Sumida
L2, L3	2		Ferrite Bead, 330 ohm @ 100 MHz, 1.5 A, 0603	0603	BLM18SG331TN1D	MuRata
L4, L5, L6	3	18µH	Inductor, Shielded, Ferrite, 18 µH, 0.12 A, 3.3 ohm, SMD		CMH322522-180KL	Bourns
Q1	1		Transistor, PNP, 40 V, 0.2 A, SOT-23	SOT-23	MMBT3906-7-F	Diodes Inc.
Q2	1		MOSFET, P-CH, -20 V, -20 A, SON 2x2mm	SON 2x2mm	CSD25310Q2	Texas Instruments
R1, R13, R16, R17, R19, R21, R23, R28, R29, R31	10	0Ω	RES, 0, 5%, 0.125 W, 0805	0805	CRCW08050000Z0EA	Vishay-Dale

R2, R7	1	499kΩ	RES, 499 k, 1%, 0.1 W, 0603	0603	CRCW0603499KFKEA	Vishay-Dale
R3	1	1.10MΩ	RES, 1.10 M, 1%, 0.1 W, 0603	0603	CRCW06031M10FKEA	Vishay-Dale
R4	1	1.00MΩ	RES, 1.00 M, 1%, 0.063 W, 0402	0402	CRCW04021M00FKED	Vishay-Dale
R5	1	200Ω	RES, 200, 1%, 0.1 W, 0603	0603	CRCW0603200RFKEA	Vishay-Dale
R6	1	196kΩ	RES, 196 k, 1%, 0.1 W, 0603	0603	CRCW0603196KFKEA	Vishay-Dale
R8	1	10.0kΩ	RES, 10.0 k, 1%, 0.1 W, 0603	0603	CRCW060310K0FKEA	Vishay-Dale
R9, R20, R22	3	1.0kΩ	RES, 1.0 k, 5%, 0.063 W, 0402	0402	CRCW04021K00JNED	Vishay-Dale
R10	1	10.0Ω	RES, 10.0, 1%, 0.1 W, 0603	0603	CRCW060310R0FKEA	Vishay-Dale
R11, R12	2	4.7kΩ	RES, 4.7 k, 5%, 0.063 W, 0402	0402	CRCW04024K70JNED	Vishay-Dale
R14, R15, R25	3	0Ω	RES, 0, 5%, 0.1 W, 0603	0603	CRCW06030000Z0EA	Vishay-Dale
R18	1	47kΩ	RES, 47 k, 5%, 0.063 W, 0402	0402	CRCW040247K0JNED	Vishay-Dale
R24	1	0Ω	RES, 0, 5%, 0.25 W, 1206	1206	CRCW12060000Z0EA	Vishay-Dale
R26	0	0Ω	RES, 0, 5%, 0.1 W, 0603	0603	CRCW06030000Z0EA	Vishay-Dale
R27, R30, R33	3	300Ω	RES, 300, 5%, 0.1 W, 0603	0603	CRCW0603300RJNEA	Vishay-Dale
R32, R34	0	0Ω	RES, 0, 5%, 0.125 W, 0805	0805	CRCW08050000Z0EA	Vishay-Dale
S1	1		Switch, Slide, SPDT, 0.2A, GULL, 12V, SMD		CL-SB-12B-01T	Copal Electronics

S2	1		Switch, Tactile, SPST-NO, 0.05A, 12V, SMT		4-1437565-1	TE Connectivity
TP1, TP2, TP3, TP4, TP5, TP6, TP7, TP8	8		Test Point, Miniature, SMT		5015	Keystone
U1	1		Adjustable, 1.8-A Switch, 96% Efficient Boost Converter with Down-Mode, DRC0010J	DRCR	TPS61029DRCR	Texas Instruments
U2	1		Mixed Signal Microcontroller, RGZ0048B	IRGZR	MSP430FR5969IRGZR	Texas Instruments
U3	1		Multi-Channel 12/26-Bit Capacitance to Digital Converter (FDC) for Capacitive Sensing, RGH0016A	RGHR	FDC2214RGHR	Texas Instruments
Y1	1		OSC, 40 MHz, 1.6 to 3.63 V, SMD		KC2520B40.0000C10E00	AVX

9.3 Layout Plots

To download the Layout Plots, see the design files at TIDA-00466.

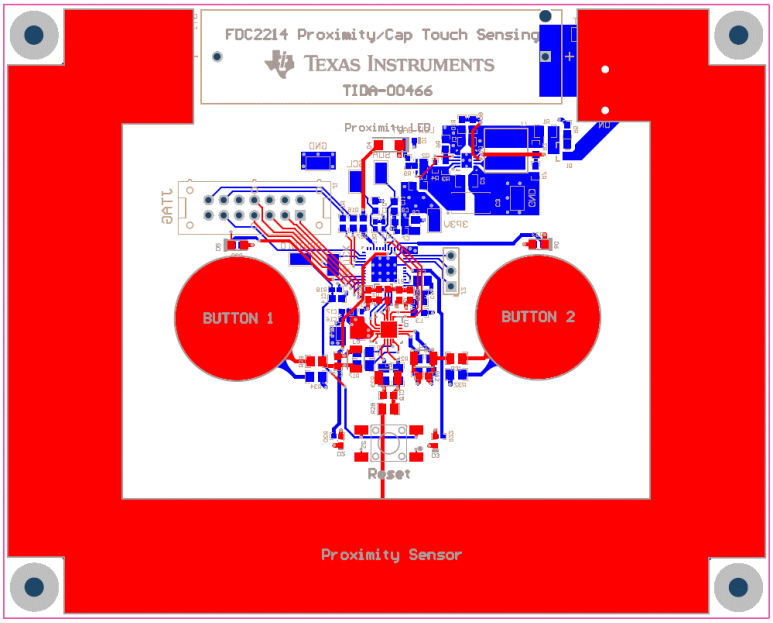

Figure 23: Composite Top and Bottom layer plot (viewed from the top)

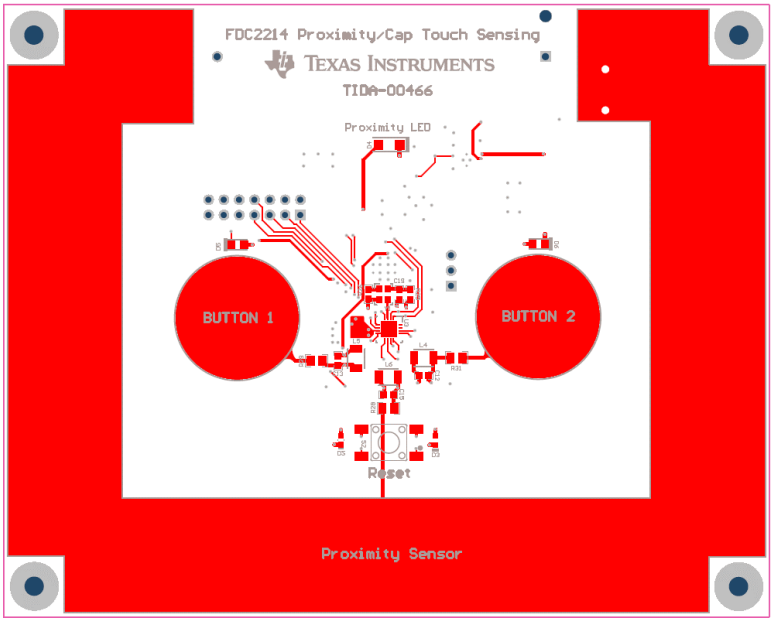

Figure 24: Top Layer

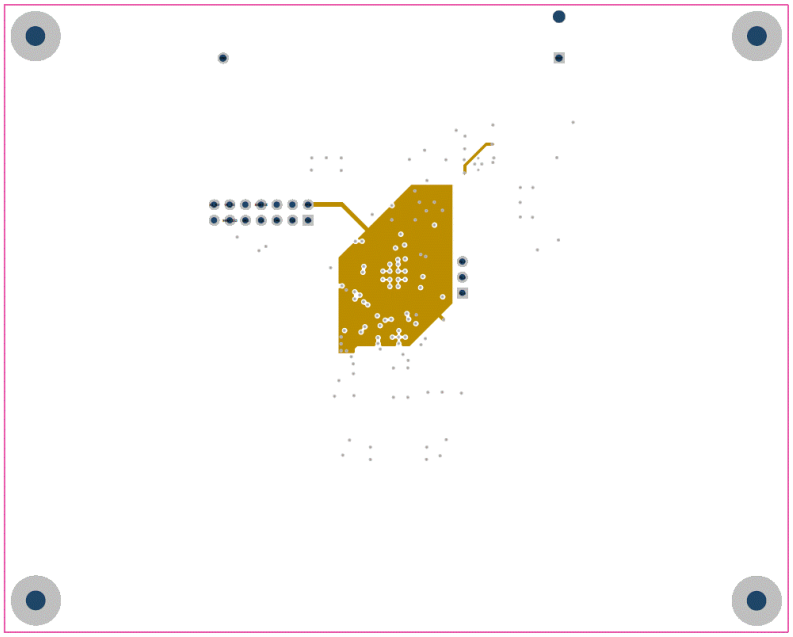

Figure 25: Midlayer 1 (Power Plane)

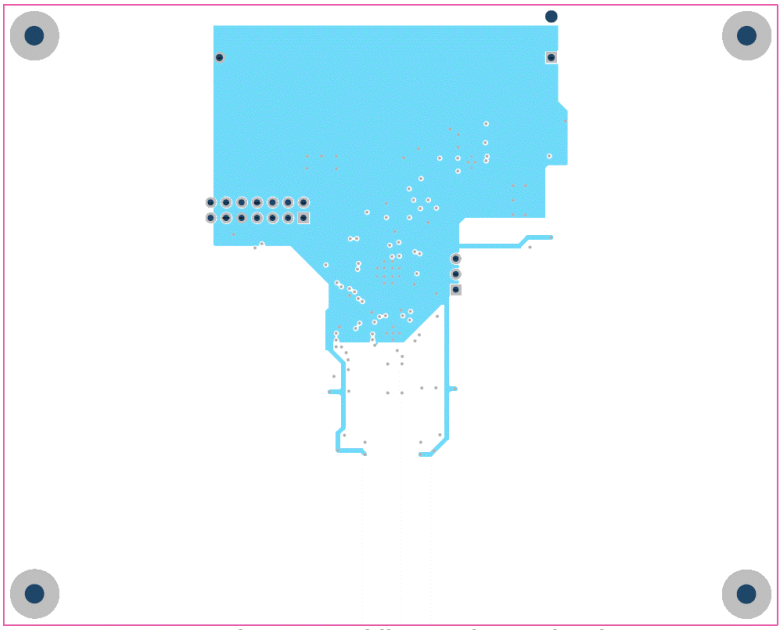

Figure 26: Midlayer 2 (GND Plane)

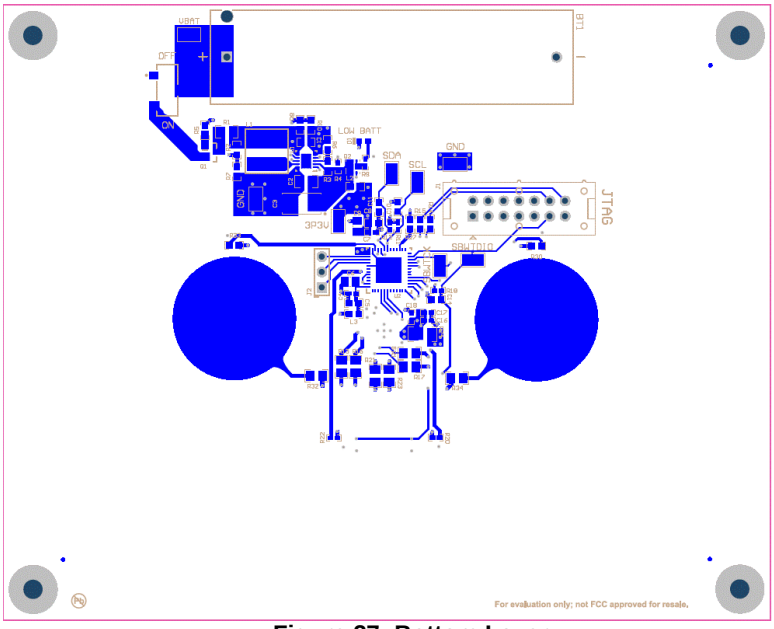

Figure 27: Bottom Layer

9.4 Layout Guidelines

- Avoid long signal traces from the FDC to the sensors. Short traces reduce parasitic capacitances and offer higher system performance.
- The signal traces should be between 10-20mils. Wider traces decrease the resistance along signal path and increases system performance.
- Systems that require matched channel response need to have matched trace length on all active channels.
- Minimize the amount of ground planes around the sensor signal traces and the sensor itself. Ground sources will reduce sensitivity of the system significantly especially if it is located on the underside of the sensor.

9.5 Gerber files

To download the Gerber files for each board, see the design files at TIDA-00466.

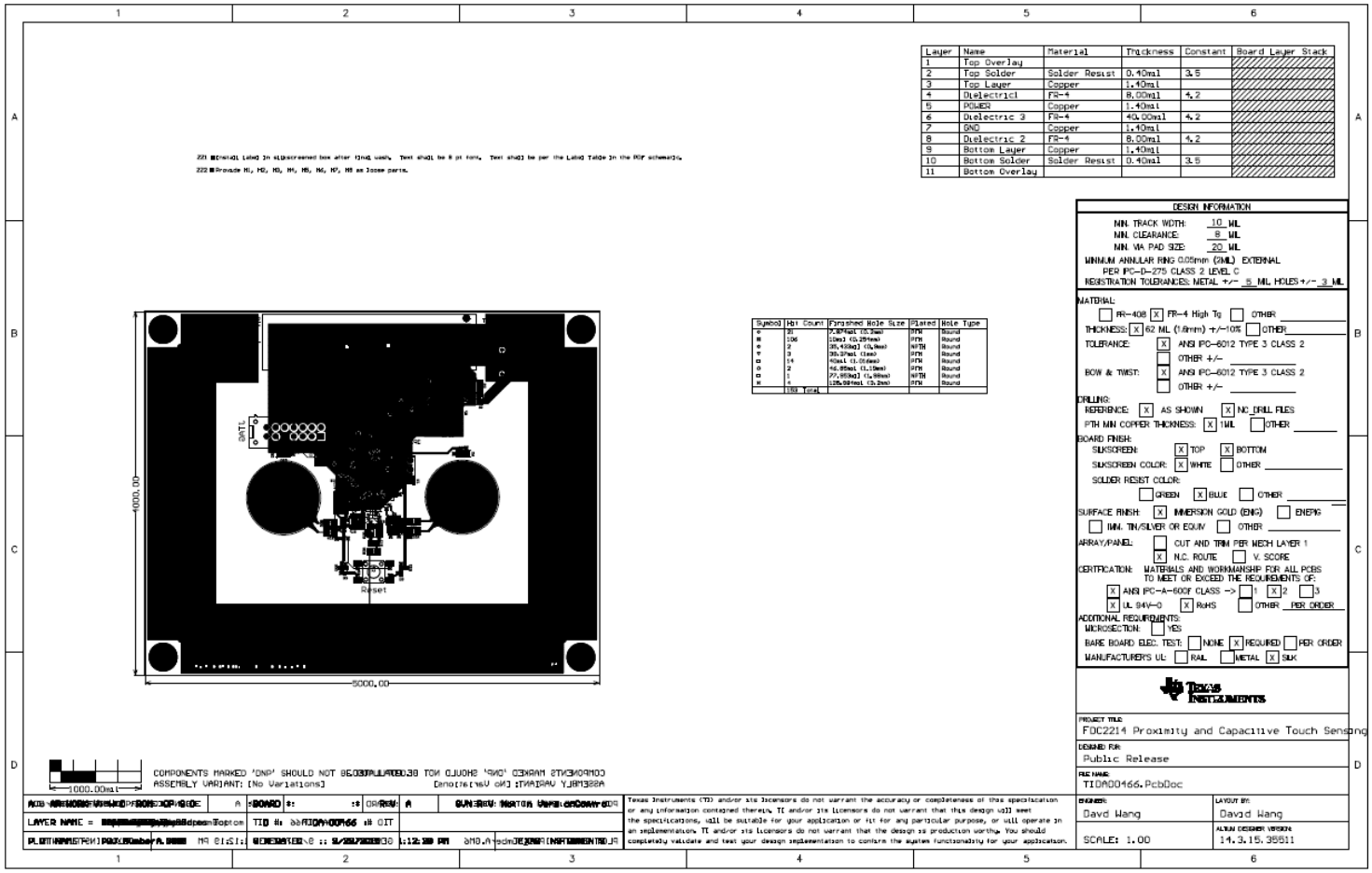

Figure 28: Gerber Files

10 References

1. Capacitive Proximity Sensing using the FDC2x1y (SNOA940)

11 Firmware

To download the MSP430 firmware source code for this TI Design, see the design files at TIDA-00466.

12 About the Author

David Wang is an Applications Engineer at Texas Instruments, where he is responsible for developing and supporting capacitive sensing solutions and technology. David brings to this role his experience in system-level design and integration expertise. David earned his Bachelors of Science in Electrical Engineering (BSEE) from the University of Florida in Gainesville, FL and Masters of Science in Electrical Engineering (MSEE) from Stanford University in Stanford, CA.

IMPORTANT NOTICE FOR TI REFERENCE DESIGNS

Texas Instruments Incorporated ("TI") reference designs are solely intended to assist designers (“Buyers”) who are developing systems that incorporate TI semiconductor products (also referred to herein as “components”). Buyer understands and agrees that Buyer remains responsible for using its independent analysis, evaluation and judgment in designing Buyer’s systems and products.

TI reference designs have been created using standard laboratory conditions and engineering practices. **TI has not conducted any testing other than that specifically described in the published documentation for a particular reference design.** TI may make corrections, enhancements, improvements and other changes to its reference designs.

Buyers are authorized to use TI reference designs with the TI component(s) identified in each particular reference design and to modify the reference design in the development of their end products. HOWEVER, NO OTHER LICENSE, EXPRESS OR IMPLIED, BY ESTOPPEL OR OTHERWISE TO ANY OTHER TI INTELLECTUAL PROPERTY RIGHT, AND NO LICENSE TO ANY THIRD PARTY TECHNOLOGY OR INTELLECTUAL PROPERTY RIGHT, IS GRANTED HEREIN, including but not limited to any patent right, copyright, mask work right, or other intellectual property right relating to any combination, machine, or process in which TI components or services are used. Information published by TI regarding third-party products or services does not constitute a license to use such products or services, or a warranty or endorsement thereof. Use of such information may require a license from a third party under the patents or other intellectual property of the third party, or a license from TI under the patents or other intellectual property of TI.

TI REFERENCE DESIGNS ARE PROVIDED "AS IS". TI MAKES NO WARRANTIES OR REPRESENTATIONS WITH REGARD TO THE REFERENCE DESIGNS OR USE OF THE REFERENCE DESIGNS, EXPRESS, IMPLIED OR STATUTORY, INCLUDING ACCURACY OR COMPLETENESS. TI DISCLAIMS ANY WARRANTY OF TITLE AND ANY IMPLIED WARRANTIES OF MERCHANTABILITY, FITNESS FOR A PARTICULAR PURPOSE, QUIET ENJOYMENT, QUIET POSSESSION, AND NON-INFRINGEMENT OF ANY THIRD PARTY INTELLECTUAL PROPERTY RIGHTS WITH REGARD TO TI REFERENCE DESIGNS OR USE THEREOF. TI SHALL NOT BE LIABLE FOR AND SHALL NOT DEFEND OR INDEMNIFY BUYERS AGAINST ANY THIRD PARTY INFRINGEMENT CLAIM THAT RELATES TO OR IS BASED ON A COMBINATION OF COMPONENTS PROVIDED IN A TI REFERENCE DESIGN. IN NO EVENT SHALL TI BE LIABLE FOR ANY ACTUAL, SPECIAL, INCIDENTAL, CONSEQUENTIAL OR INDIRECT DAMAGES, HOWEVER CAUSED, ON ANY THEORY OF LIABILITY AND WHETHER OR NOT TI HAS BEEN ADVISED OF THE POSSIBILITY OF SUCH DAMAGES, ARISING IN ANY WAY OUT OF TI REFERENCE DESIGNS OR BUYER’S USE OF TI REFERENCE DESIGNS.

TI reserves the right to make corrections, enhancements, improvements and other changes to its semiconductor products and services per JESD46, latest issue, and to discontinue any product or service per JESD48, latest issue. Buyers should obtain the latest relevant information before placing orders and should verify that such information is current and complete. All semiconductor products are sold subject to TI’s terms and conditions of sale supplied at the time of order acknowledgment.

TI warrants performance of its components to the specifications applicable at the time of sale, in accordance with the warranty in TI’s terms and conditions of sale of semiconductor products. Testing and other quality control techniques for TI components are used to the extent TI deems necessary to support this warranty. Except where mandated by applicable law, testing of all parameters of each component is not necessarily performed.

TI assumes no liability for applications assistance or the design of Buyers’ products. Buyers are responsible for their products and applications using TI components. To minimize the risks associated with Buyers’ products and applications, Buyers should provide adequate design and operating safeguards.

Reproduction of significant portions of TI information in TI data books, data sheets or reference designs is permissible only if reproduction is without alteration and is accompanied by all associated warranties, conditions, limitations, and notices. TI is not responsible or liable for such altered documentation. Information of third parties may be subject to additional restrictions.

Buyer acknowledges and agrees that it is solely responsible for compliance with all legal, regulatory and safety-related requirements concerning its products, and any use of TI components in its applications, notwithstanding any applications-related information or support that may be provided by TI. Buyer represents and agrees that it has all the necessary expertise to create and implement safeguards that anticipate dangerous failures, monitor failures and their consequences, lessen the likelihood of dangerous failures and take appropriate remedial actions. Buyer will fully indemnify TI and its representatives against any damages arising out of the use of any TI components in Buyer’s safety-critical applications.

In some cases, TI components may be promoted specifically to facilitate safety-related applications. With such components, TI’s goal is to help enable customers to design and create their own end-product solutions that meet applicable functional safety standards and requirements. Nonetheless, such components are subject to these terms.

No TI components are authorized for use in FDA Class III (or similar life-critical medical equipment) unless authorized officers of the parties have executed an agreement specifically governing such use.

Only those TI components that TI has specifically designated as military grade or “enhanced plastic” are designed and intended for use in military/aerospace applications or environments. Buyer acknowledges and agrees that any military or aerospace use of TI components that have ***not*** been so designated is solely at Buyer's risk, and Buyer is solely responsible for compliance with all legal and regulatory requirements in connection with such use.

TI has specifically designated certain components as meeting ISO/TS16949 requirements, mainly for automotive use. In any case of use of non-designated products, TI will not be responsible for any failure to meet ISO/TS16949.

Mailing Address: Texas Instruments, Post Office Box 655303, Dallas, Texas 75265